

Structural, optical and electrical characterization of MoS₂/TiO₂ heterostructured thin films by chemical bath deposition technique

M. I. Khan^{a,*}, H. Nouman^a, M. Ul Hassan^a, S. Ul Hasan^a, A. Nazneen^a, Shaimaa A. M. Abdelmohsen^b

^a*Department of Physics, The University of Lahore, Pakistan*

^b*Department of Physics, College of Science, Princess Nourah bint Abdulrahman university. P.O. Box 84428, Riyadh 11681, Saudi Arabia*

MoS₂/TiO₂ heterostructures thin films are successfully deposited by chemical bath deposition (CBD) technique. The structural, optical and electrical properties of prepared films are characterized by X-ray diffraction (XRD), Raman spectroscopy, UV-vis spectrophotometry, photoluminescence spectroscopy (PL), and Four point probe technique, respectively. Raman Spectra and XRD confirmed the formation of hexagonal MoS₂ and anatase TiO₂. UV-Vis spectrophotometry confirmed the band gap energy (E_g) of MoS₂ and TiO₂ thin films are 1.14 eV and 3.44 eV, respectively. The E_g of films is changed according to the material deposited onto them i.e. it increased by depositing TiO₂ onto the MoS₂ and decreased the other way round. MT (Titania on Molybdenum disulfide) and TM (Vice Versa) have band gaps of 2.81 eV and 1.5 eV, respectively. The photoluminescence spectra showed that photoluminescence emission increased for TiO₂ in the MoS₂/TiO₂ and TiO₂/MoS₂ heterostructures films. The exchange of trion to neutral excitons by charges transfer from MoS₂ to TiO₂ in heterostructures leads to increase the PL intensity. The average sheet resistivity of TiO₂, MoS₂, glass/MoS₂/TiO₂ and glass/TiO₂/MoS₂ films are 2.41×10^7 (Ω -m), 6.44×10^4 (Ω -m), 1.93×10^6 (Ω -m) and 2.35×10^4 (Ω -m), respectively. CBD is low cost, simple, and large area deposition technique and by this research the heterostructures films can easily be deposited for industrial purpose.

(Received July 28, 2021; Accepted February 2, 2022)

Keywords: TiO₂, MoS₂, Heterostructures, Chemical bath deposition

1. Introduction

The major problems facing mankind today are the increase of consumption of energy and pollution. Therefore, the utilization of solar energy has gained much attention to overcome these problems [1, 2]. Considering their unique design, low cost, and outstanding physicochemical characteristics, both MoS₂ and TiO₂ are very interesting photocatalyst [3-5]. TiO₂ is considered a good photocatalyst due to its versatility, non-toxicity, stability, and environmental friendliness [6, 7]. MoS₂ is a two-part graphene-like material and is a promising character for the construction of heterojunction with TiO₂ sites due to its high oxidation function and strong transfer capability [8]. Graphene has unusual characteristics like good electrical, optical, mechanical and thermal properties. It has high carrying capacity, high flexibility and good stability [9-11]. While most 2D transition metal dichalcogenides (TMDs) have huge variation in electronic structures, which depend on the numbers of layers. TMDs in bulk form have indirect bandgap, and in layer form have direct bandgap, which provides a good variety of uses. Among other TMDs, monolayer of MoS₂ has attracted much attention of researcher due to its direct band of ~ 1.90 eV, which absorbs light of ~ 652 nm falling over a visible distance, resulting in fine photoluminescence (PL) and a highly good response of optoelectronics in its own unique way [12-14]. However, this is a milestone, the task of achieving high and strong PL emissions from single layer of MoS₂, the tuning and correction of the optical characteristics is acceptable as an option [15-18]. 1L-MoS₂ can

* Corresponding author: iftikharphysicsuet@gmail.com

<https://doi.org/10.15251/CL.2022.192.75>

be tuned to a depth of PL, with the help of intercept with different materials (plasmonic, TMDs etc.). MoS₂ is said to primarily shape diversity in their interfaces with giant bandgap (UV energetic) semiconductors such as ZnO and TiO₂, which is precisely the nano-enhanced structure that facilitates separation of charges and low PL emissions. In particular, the MoS₂/TiO₂ heterostructures is known for its excellent composite optical housing due to their high chemical balance and abundance. Therefore, those types of heterostructures are very promising for programs in many fields, including photoelectric gadgets, energy conversion, photocatalysis, and environmental programs [3, 19-26].

The low cost, easy fabrication and large area deposition thin films are industry requirement. Thin films can be deposited by pulse laser deposition [27], magnetron sputtering [28], sol-gel [29], and chemical bath deposition technique [30]. Among all these techniques, CBD is low cost and large area deposition technique. This technique is very useful for industry purpose.

Here we report a synthesis and characterization of TiO₂ and MoS₂ prepared by CBD technique. The PL intensity of MoS₂ is increased after the formation of heterostructures. This increment is due to the conversion of trions into neutral species. XRD and Raman spectroscopy confirmed the formation of hexagonal MoS₂ and anatase TiO₂. UV-vis spectrophotometry shows band gap of the films changed according to the material deposited onto them i.e. it increased by adding TiO₂ onto the MoS₂ and vice versa.

2. Experimental Setup

Thin films of TiO₂, MoS₂, glass/MoS₂/TiO₂ and glass/TiO₂/MoS₂ were deposited via CBD technique on glass substrates. Dissolution of water and titanium nitrate (Ti(NO₃)₄) were stoichiometrically poured into the mixture of citric acid solution. 24 ml ammonia (HNO₃) was added in 8 ml distilled water and continuous stirring was performed until the solution was formed. This new formed solution was inserted into the afore formed solutions. This solution was sterilized for three hours. For the formation of MoS₂ solution; 4.32 g MoO₃ dissolute was made in distilled water and 2.28 g Thiourea was added into the solution under continuous stirring. 24 ml ammonia (HNO₃) was added in 8 ml distilled water to make solution with continuous hand stirring. Both solutions were added and the whole solution was sterilized for 4 hrs until the blackish gray gel was formed. The above solutions were used for the deposition of TiO₂, MoS₂, glass/MoS₂/TiO₂ and glass/TiO₂/MoS₂ by CBD technique. The chemically washed glass slides were inserted vertically into the solution of TiO₂ for 90 min. After that, the film was annealed at 100 °C for 10 minutes. After that film was annealed at 450 °C for 2 hours. Similarly, glass slide was inserted vertically into the solution of MoS₂ for 90 min and annealed at 100 °C for 10 minutes. Now the nanoparticles are formed from the solution of TiO₂ and annealed these particles at 450 °C. These nanoparticles are added in ethanol for forming the solution of TiO₂. On the same above method repeated for the deposition of glass/TiO₂/MoS₂ and glass/MoS₂/TiO₂ films.

2.1. Characterization Techniques

Various characterization techniques were employed to attain the characteristics of synthesized materials including XRD, Raman, UV-Vis and Photoluminescence. Panalytical X'celerator detector and Cu K α radiation ($\lambda=1.54056\text{\AA}$) was employed for XRD analysis. Structural and Vibrational modes were determined by Raman spectroscopy. UV-vis technique was applied to investigate optical properties. In order to evaluate the electronic transitions in terms of associated photons photoluminescence was employed as technique. Electrical properties were measured by four point probe (KIETHLEY Instrument) technique.

3. Results and discussions

3.1. Structural Analysis

The Phase structures of as-prepared samples are investigated by XRD with a panalytical X'celerator detector and Cu K α radiation ($\lambda=1.54056\text{\AA}$). The XRD patterns of MoS₂, TiO₂-MoS₂,

TiO₂, and MoS₂-TiO₂ sample are shown in Figure 1. For pure MoS₂ all the diffraction peaks appeared at $2\theta = 33.3^\circ$, 41.1° and 58.31° , which are assigned to (100), (103) and (110) lattice-planes, respectively. These three diffraction peaks showed the hexagonal phases of MoS₂ (PDF Card-No 17-0744) [31-33]. For pure TiO₂ all diffraction peaks appeared at $2\theta = 25.28^\circ$, 37.80° , and 48.04° matching to (101), (004) and (200) lattice-planes of anatase-phase of TiO₂ (PDF Card-No 21-1272) [31]. The XRD pattern of TiO₂-MoS₂ stacking its MoS₂ for which the peaks are more pronounced whereas in MoS₂-TiO₂ stacking its TiO₂ showing more pronounced peaks. So results showed that 2H-MoS₂/TiO₂ structure were fruitfully synthesized. Excitingly, all diffraction peaks of TiO₂ and MoS₂ are existed in XRD. But, peaks intensities are decreased and MoS₂ peaks are shifted slightly to the right. This shift is attributed to existing of different stress on MoS₂ when nanosheets of MoS₂ were grown into a thin film of TiO₂. Therefore, TiO₂ can inhibit the growth of MoS₂ crystals [34].

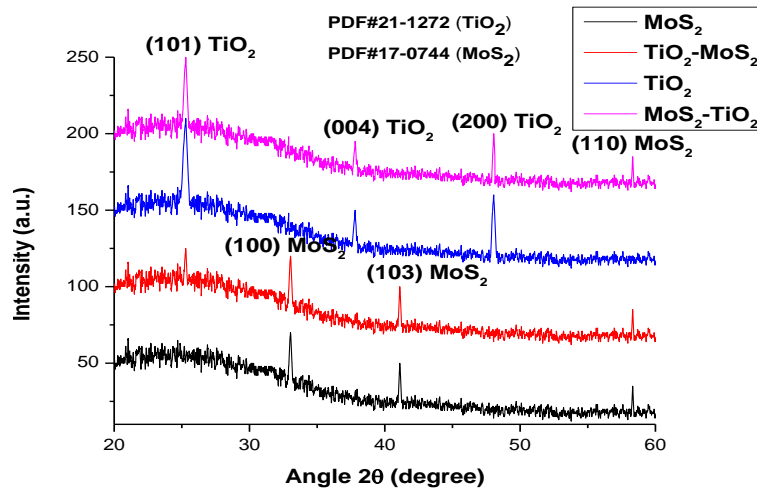


Fig. 1. XRD patterns of MoS₂, TiO₂, TiO₂-MoS₂, and MoS₂-TiO₂.

The calculated parameters of fabricated materials are mentioned in Table 1. The parameters of interest were evaluated using Debye Scherrer's Relation as,

$$S = K \frac{\lambda}{\beta \cos\theta} \quad (1)$$

where, S is the crystallite size. β represents the diffraction peak measured at a full width half maxima (FWHM). Dislocation density was computed using the relation as,

$$D = \frac{1}{S^2} \quad (2)$$

Table 1. Summary of XRD results.

Samples	2θ (Degree)	Avg. Grain Size (nm)	Dislocation Density (10^{17})	d-spacing (Å)	(hkl)	Lattice parameters (Å)
TiO ₂	25.28	34.7	0.0166	3.52	(101)	a = 3.79, c = 9.52
MoS ₂	33.03	43.76	0.0048	2.71	(100)	a = 3.16, c = 1.92
MoS ₂ - TiO ₂	25.28	66.76	0.0166	3.52	(101)	
TiO ₂ - MoS ₂	25.28	34.7	0.0166	3.52	(101)	

It can be seen from the Figure 2 that the average grain size of titania is not changed noticeably when MoS₂ was grown onto it but in case of MoS₂ it decreased quite much when titania was grown onto it. Reducing grain size enhanced the surface area, mean improved the photocatalytic activity [35, 36].

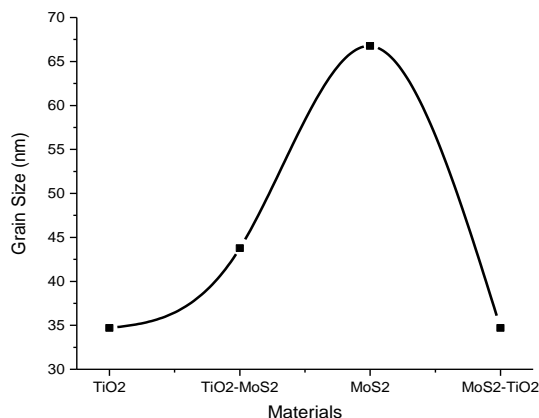


Fig. 2. Comparison of Grain Size.

The largest value of inter-planar spacing realized to be in perfect agreement with previous work for all the films. The broader peaks in the X-ray diffraction pattern shown here suggested the occurrence of very small crystallites [37].

3.2. Raman Analysis

Structural and vibrational modes of nanoparticles are characterized by Raman spectroscopy. The spectra of MoS₂, TiO₂, glass/MoS₂/TiO₂ and glass/TiO₂/MoS₂ are shown in Figure 3. For pure MoS₂ seven peaks are formed at 129, 151, 285, 337, 663, 818 and 996. The 1st order Raman band of 2H-MoS₂ is located at 285 (E_{1g}), this active mode is a forbidden mode in backscattering experimentation basal plane [38]. Due to distorted structure low frequency vibrational modes also appeared at 337(A_g) and 151(B_g). However, at high laser power excitation the drastic alterations took place in Raman spectrum with solid peaks appeared at 818 and 996 cm⁻¹, representing the molybdenumoxide. Strong band described to the Mo–O–Mo enlarging vibration helps as a suitable marker for judgement of orthorhombic (818 cm⁻¹) and (996 cm⁻¹) crystal phases. The evidently defined peaks at 129, 151, 285, 337, 663, 818, and 996 cm⁻¹ are strong evidence for laser induced formation of Orthorhombic MoO₃ [2, 14, 39].

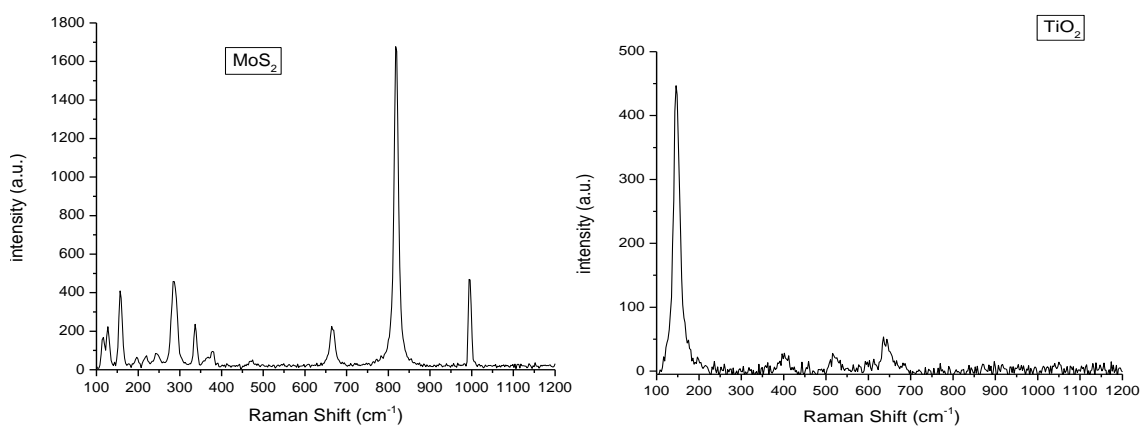


Fig. 3.1 Raman Spectra of MoS₂, TiO₂.

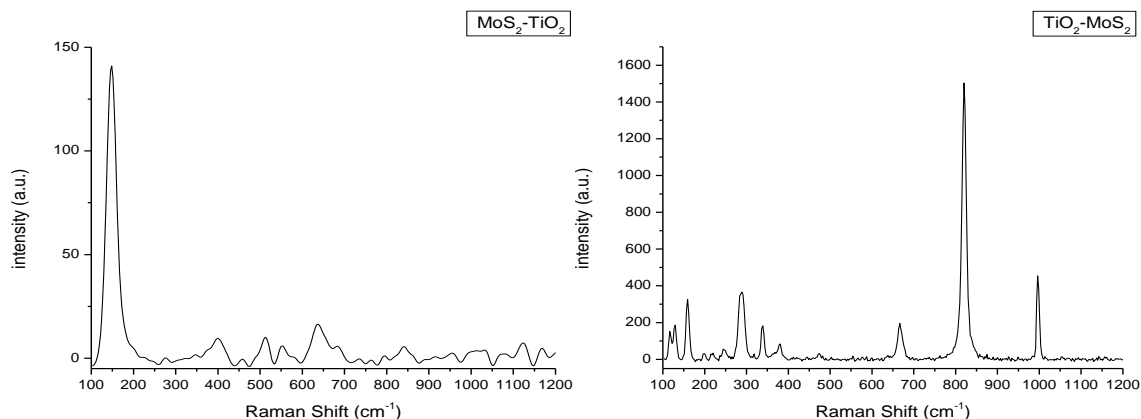


Fig. 3.2 Raman Spectra of $\text{MoS}_2\text{-TiO}_2$ and $\text{TiO}_2\text{-MoS}_2$.

For pure TiO_2 four peaks formed at 146, 401, 514 and 637 cm^{-1} which are the diffraction peaks of TiO_2 that coincide with anatase modes of E_g^1 , B_{1g}^1 , $A_{1g} + B_{1g}^2$ and E_g^2 [31, 40]. For $\text{MoS}_2\text{-TiO}_2$, only one peak of 2H- MoS_2 appeared at 404 cm^{-1} (A_{1g}) while other peaks at 150, 515 and 633 cm^{-1} showed the anatase phase of TiO_2 . Similarly, for $\text{TiO}_2\text{-MoS}_2$ only one peak of TiO_2 appeared at 154 while other peaks at 129, 288, 341, 337, 666, 819 and 996 cm^{-1} demonstrated MoS_2 [2, 31, 39, 40]. It concludes that for $\text{TiO}_2\text{-MoS}_2$: the MoS_2 peaks are more pronounced whereas in $\text{MoS}_2\text{-TiO}_2$, the TiO_2 peaks are more pronounced. Hence, these results indicated the presence of 2H- MoS_2 and anatase phase of TiO_2 .

3.3. UV visible spectroscopy for Band gap evaluation

UV visible spectroscopy was employed to compute the bandgap energy (E_g) of prepared specimen. Figure (4) represented the Tauc's plot for titania and MoS_2 . From Figure 4, Band gap energy for pure titania and pure MoS_2 is 3.44 eV and 1.14 eV, respectively. Such small band gap energy demonstrated by MoS_2 depicted itself to be active in the photo activity [34]. The measured bandgap energy values for both synthesized materials are well agreed literature [34, 41].

Tauc's plot for heterostructure stackings M-T and T-M are also included in Figures 4, respectively. The band gap for MT configuration was 2.80 whereas for TM it was 1.5 eV. It was realized that adding of MoS_2 in titania decreased the band gap energy of the stacked layers overall, while addition of titania in MoS_2 showed the increased pattern. This could be attributed to smaller and greater bandgaps of the material added secondly than the firstly grown material [34].

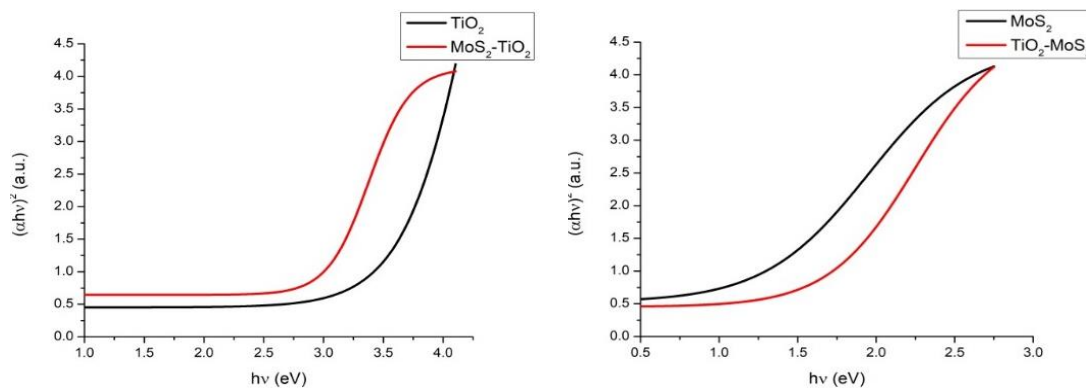


Fig. 4. Tauc's plot TiO_2 , MoS_2 and $\text{MoS}_2\text{-TiO}_2$ and $\text{TiO}_2\text{-MoS}_2$.

3.4. Photoluminescence

The photoluminescence (PL) emission spectra is used to study the performance of Photo-generated carriers. The movement of Photo-generated (e^-/h^+) pairs in $\text{MoS}_2/\text{TiO}_2$ and $\text{TiO}_2/\text{MoS}_2$ were studied by photoluminescence analysis as shown in Fig. 5.

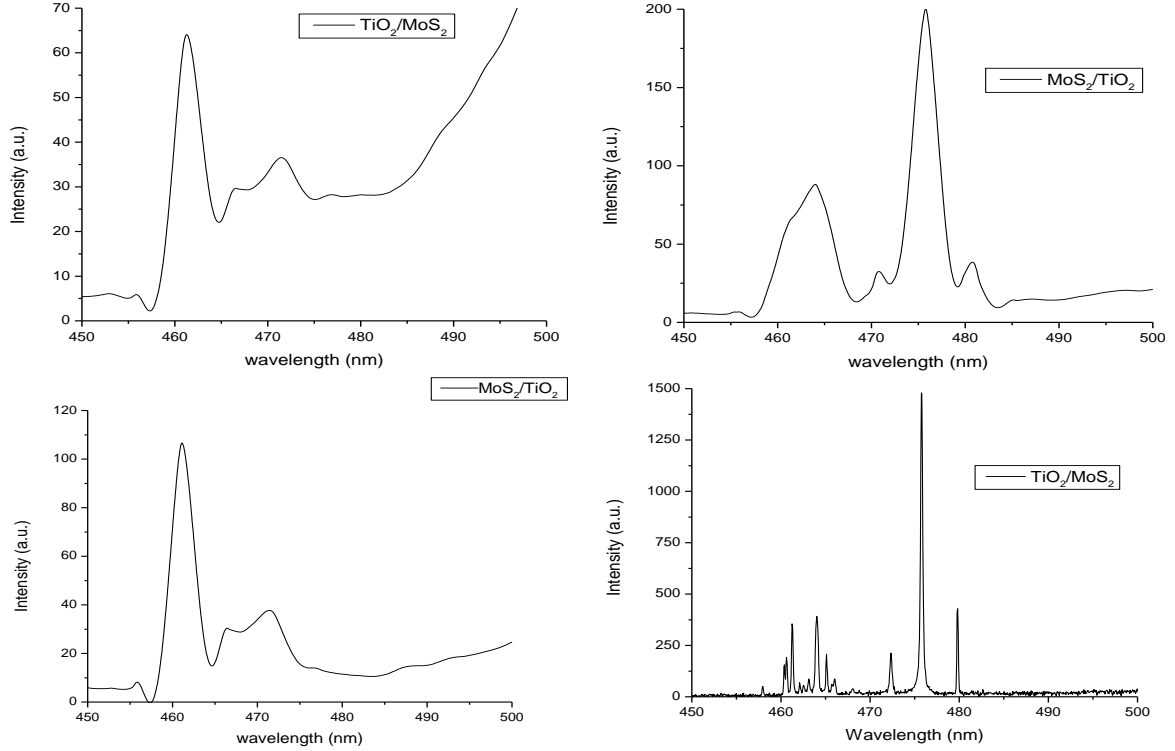


Fig. 5. PL of MoS_2 , TiO_2 , $\text{TiO}_2/\text{MoS}_2$ and $\text{MoS}_2/\text{TiO}_2$.

For pure MoS_2 one peak is formed at 463 nm having intensity 64 cm^{-1} . For pure TiO_2 two peaks are formed at 463 nm and 475 nm having intensities 88.52 cm^{-1} and 200 cm^{-1} respectively. For $\text{MoS}_2/\text{TiO}_2$ peak is formed at 463 nm having intensity 107.10 cm^{-1} . Similarly, for $\text{TiO}_2/\text{MoS}_2$ two peaks are formed at 463 nm and 475 nm having intensities 390 cm^{-1} and 1463 cm^{-1} respectively. These results show that PL intensities at 463 nm and 475 nm for heterostructures films. The exchange of trion to neutral excitons by the transfer of charges from MoS_2 to TiO_2 in heterostructure leads to increase the PL intensity [14]. TiO_2 film is annealed at 400°C . At this high temperature, Ti interstitials point and oxygen vacancies defects increased in the pure TiO_2 , leading to an increase in the defects induced PL of TiO_2 [42]. Furthermore, extra electrons may also transfer from MoS_2 to TiO_2 than recombine at TiO_2 sites. Thus the PL emission increased for TiO_2 in the $\text{MoS}_2/\text{TiO}_2$ and $\text{TiO}_2/\text{MoS}_2$ heterostructure [43].

3.5. Electrical Properties

Sheet resistivity of the film is measured by the equation (4) [29].

$$\rho = \frac{V\pi}{I(\ln 2)} \quad (4)$$

where ρ is sheet resistivity of films, I and V are current and voltage, respectively. The average sheet resistivity of TiO_2 , MoS_2 , glass/ $\text{MoS}_2/\text{TiO}_2$ and glass/ $\text{TiO}_2/\text{MoS}_2$ films are $2.41 \times 10^7 \text{ }(\Omega\text{-m})$, $6.44 \times 10^4 \text{ }(\Omega\text{-m})$, $1.93 \times 10^6 \text{ }(\Omega\text{-m})$ and $2.35 \times 10^4 \text{ }(\Omega\text{-m})$, respectively. It is observed that the sheet resistivity of bi-layered film is decreased as compared to single layered film, therefore, bi-

layered films are good for electrical applications. This variation in electrical properties is due to variation in grain size.

4. Conclusion

MoS₂/TiO₂ heterostructures thin films are prepared by CBD method. The thin films of MoS₂ and TiO₂ were found to be hexagonal and anatase phase structured, completely coinciding with the literature. The band gap energies of MoS₂ and TiO₂ films are found to be 1.14 eV and 3.44 eV, respectively. The E_g of the films changed according to the deposited of material i.e. it increased by addition of TiO₂ onto the MoS₂ and decreased the other way round. MT (Titania on Molybdenum disulfide) and TM (Vice Versa) showed the band gaps 2.81 eV and 1.5 eV, respectively. The photoluminescence spectra confirmed photoluminescence emission increased for TiO₂ in the MoS₂/TiO₂ and TiO₂/MoS₂ heterostructure. The exchange of trion to neutral excitons by charges transfer from MoS₂ to TiO₂ in heterostructure leads to increase the PL intensity. The sheet resistivity of bi-layered film is decreased as compared to single layered film. The results provided a simple way to build MoS₂-based heterostructures and it has many useful applications in opto-electronic and nano-photonic devices.

Acknowledgements

This research was funded by Princess Nourah bint Abdulrahman University Researchers Supporting Project number (PNURSP2022R61), Princess Nourah bint Abdulrahman University, Riyadh, Saudi Arabia.

References

- [1] S. Bai et al., Nano Research 8(1), 175 (2015); <https://doi.org/10.1007/s12274-014-0606-9>
- [2] F.-J. Zhang et al., Journal of the Korean Ceramic Society 56(3), 284 (2019); <https://doi.org/10.4191/kcers.2019.56.3.06>
- [3] B. Chen et al., Nanoscale 10(1), 34 (2018); <https://doi.org/10.1039/C7NR07366F>
- [4] W. Tu et al., Nanoscale 9(26), 9065 (2017); <https://doi.org/10.1039/C7NR03238B>
- [5] J. Tian et al., Chemical Society Reviews 43(20), 6920 (2014).
- [6] K. Han et al., Journal of Nanoscience and Nanotechnology 16(9), 9826 (2016); <https://doi.org/10.1166/jnn.2016.12364>
- [7] M. S. Hamdy et al., Journal of catalysis 310, 75 (2014); <https://doi.org/10.1016/j.jcat.2013.07.017>
- [8] X. Liu et al., Applied Catalysis B: Environmental 201, 119 (2017); <https://doi.org/10.1016/j.apcatb.2016.08.031>
- [9] X. Du et al., Nature nanotechnology 3(8), 491 (2008); <https://doi.org/10.1038/nnano.2008.199>
- [10] A. A. Balandin et al., Nano letters 8(3), 902 (2008); <https://doi.org/10.1021/nl0731872>
- [11] K. I. Bolotin et al., Solid state communications 146(9-10), 351 (2008); <https://doi.org/10.1016/j.ssc.2008.02.024>
- [12] K. F. Mak et al., Physical review letters 105(13), 136805 (2010); <https://doi.org/10.1103/PhysRevLett.105.136805>
- [13] D. Sarkar et al., Nature 526(7571), 91 (2015); <https://doi.org/10.1038/nature15387>
- [14] L. P. Mawlong, K. K. Paul, P. K. Giri, The Journal of Physical Chemistry C 122(26), 15017 (2018); <https://doi.org/10.1021/acs.jpcc.8b03957>
- [15] M. S. Kim et al., ACS nano 10(6), 6211 (2016); <https://doi.org/10.1021/acs.nano.6b02213>

- [16] Y. Zeng et al., *Advanced Materials Interfaces* 4(21), 1700739 (2017); <https://doi.org/10.1002/admi.201700739>
- [17] A. Sobhani et al., *Applied Physics Letters* 104(3), 031112 (2014); <https://doi.org/10.1063/1.4862745>
- [18] G. Ghimire et al., *The Journal of Physical Chemistry C* 122(12), 6794 (2018); <https://doi.org/10.1021/acs.jpcc.8b00092>
- [19] K. K. Paul, R. Ghosh, P. Giri, *Nanotechnology* 27(31), 315703 (2016); <https://doi.org/10.1088/0957-4484/27/31/315703>
- [20] K. K. Paul, P. Giri, *The Journal of Physical Chemistry C* 121(36), 20016 (2017); <https://doi.org/10.1021/acs.jpcc.7b05328>
- [21] Y.-H. Tan et al., *Journal of Applied Physics* 116(6), 064305 (2014); <https://doi.org/10.1063/1.4893020>
- [22] Y. Sun et al., *Inorganic Chemistry Frontiers* 5(1), 145 (2018); <https://doi.org/10.1039/C7QI00491E>
- [23] S. Mondal, D. Basak, *Applied Surface Science* 427, 814 (2018); <https://doi.org/10.1016/j.apsusc.2017.08.037>
- [24] S. Mondal, D. Basak, *Journal of Luminescence* 179, 480 (2016); <https://doi.org/10.1016/j.jlumin.2016.07.046>
- [25] S. Sarkar, D. Basak, *ACS applied materials & interfaces* 7(30), 16322 (2015); <https://doi.org/10.1021/acsami.5b03184>
- [26] K. Paul, P. Giri, Plasmonic metal and semiconductor nanoparticle decorated TiO₂-based photocatalysts for solar light driven photocatalysis, 2018; <https://doi.org/10.1016/B978-0-12-409547-2.13176-2>
- [27] V. Vaithianathan et al., *Journal of crystal growth* 287(1), 85 (2006); <https://doi.org/10.1016/j.jcrysgro.2005.10.048>
- [28] L.-W. Lai, C.-T. Lee, *Materials Chemistry and Physics* 110(2), 393 (2008); <https://doi.org/10.1016/j.matchemphys.2008.02.029>
- [29] M. Khan et al., *Results in Physics* 7, 651 (2017); <https://doi.org/10.1016/j.rinp.2016.12.029>
- [30] A. Elfanaoui et al., *Moroccan Journal of Condensed Matter* 13(3), 2011.
- [31] H. Fan et al., *Journal of Materials Science* 53(14), 10302 (2018); <https://doi.org/10.1007/s10853-018-2266-8>
- [32] D. Xie et al., *Chemistry-A European Journal* 22(33), 11617 (2016); <https://doi.org/10.1002/chem.201601478>
- [33] J. Pei et al., *Nanoscale* 10(36), 17327 (2018); <https://doi.org/10.1039/C8NR05451G>
- [34] H. N. T. Phung et al., *Journal of Nanomaterials*, 2017.
- [35] I. J. Badovinac et al., *Thin Solid Films* 709, 138215 (2020); <https://doi.org/10.1016/j.tsf.2020.138215>
- [36] M. Maeda, T. Watanabe, *Surface and Coatings Technology* 201(22-23), 9309 (2007); <https://doi.org/10.1016/j.surfcoat.2007.04.094>
- [37] T. Theivasanthi, M. Alagar, Titanium dioxide (TiO₂) nanoparticles XRD analyses: an insight. arXiv preprint arXiv:1307.1091, 2013.
- [38] A. Nazneen et al., *Journal of Molecular Structure* 1220, 128735 (2020); <https://doi.org/10.1016/j.molstruc.2020.128735>
- [39] A. Jagminas et al., *Scientific reports* 6, 37514 (2016); <https://doi.org/10.1038/srep37514>
- [40] R. Wei et al., *Optics Express* 24(22), 25337 (2016); <https://doi.org/10.1364/OE.24.025337>
- [41] A. Dashora, U. Ahuja, K. Venugopalan, *Computational materials science* 69, 216 (2013); <https://doi.org/10.1016/j.commat.2012.11.062>
- [42] B. Santara et al., *Journal of Physics D: Applied Physics* 47(21), 215302 (2014); <https://doi.org/10.1088/0022-3727/47/21/215302>
- [43] L. P. Mawlong, K. K. Paul, P. Giri, *AIP Conference Proceedings*, 2019, AIP Publishing LLC.